Neural prediction of water absorption in the sealing process of a dam grout curtain

Marek Słoński and Zenon Waszczyszyn

Cracow University of Technology, Department of Computer Methods in Civil Engineering,
ul. Warszawska 24, 31-155 Kraków, Poland
e-mail: {mslonski, zenwa}@twins.pk.edu.pl

Abstract

The problem is formulated as a prediction of unit water absorption Q in secondary boreholes on the base of measurements of the unit water and cement absorption in primary boreholes. Having a predicted water absorption Q the injection of cement grout can be evaluated. The paper is associated with measurements carried out on the earth dam Klimkówka in the South-Eastern Poland. The input and output data correspond to average values of measured unit absorption in three curtain layers. Back Propagation Neural Networks (BPNNs) and Fuzzy Weight Neural Networks (FWNNs) were used in each layer. It was stated that satisfactory crisp approximation was achieved in the deepest layer C. Application of FWNNs gave interval type predictions in all layers.

Keywords: dam grout curtain, layer of curtain, unit water absorption, Back Propagation Neural Network, Fuzzy Weight NN

1 Introduction

1.1 Problem description

One of the most important element of water reservoir is a grout curtain below the dam. The main goal of the grout curtain is to reduce seepage through the foundation of dam. The grout curtain is developed by the injection of pumpable materials into the soil foundation. The necessity of grouting is mainly derived from the results of water pressure tests (WPTs). During the WPT water is pressed into the joints and the amount of water absorbed is measured. The absorption of 1 liter of water per minute and per 1 m of borehole under pressure of 1 MPa makes 1 Lugeon (1 Lu) [1]. If the amount of water absorbed in the particular borehole is greater than a limit value then the injection of cement grout into a soil or rock formation is performed. Firstly, the injection is performed in regularly spaced (10 m) primary boreholes. Secondly, the injection is continued in secondary boreholes which are located half way between primary boreholes. The injection is performed also in tertiary and quaternary boreholes (if more boreholes are required) [2]. The technology of grouting described above is very time-consuming and expensive. This is mainly caused by making secondary boreholes and carrying out WPTs in them. That is why Artificial Neural Networks (ANNs) are used to predict the water absorption in secondary boreholes without WPTs.

1.2 Klimkówka dam grout curtain

A neural prediction approach is discussed on the earth dam Klimkówka on the Ropa river in the South-Eastern Poland [3]. In Fig. 1. a scheme of grout curtain is shown. The curtain is divided into three layers A, B, C independent of the basement soil stratification. Two primary exemplified boreholes Nos 109, 117 are marked as solid vertical lines and the secondary borehole No 113 is shown by dashed line. Altogether 34 primary boreholes were performed in which WPTs were made and cement injection was made. The same was repeated for 33 secondary boreholes. On the basis of evidence of measurements during the sealing process [3] a data set of patterns could be selected corresponding to the following input vector $\mathbf{x}$ and a scalar output y:

$$\mathbf{x} = \{q_L, q_R, c_L, c_R\}, \quad y = Q, \tag{1}$$

where: q_L, q_R – the unit water absorptions in the left and right hand sides boreholes L and R, respectively; c_L, c_R – unit cement grout absorption in the boreholes L and R; Q – unit water absorption in the secondary borehole between L and R.

Altogether $P = 74$ patterns could be completed with the distribution $PA = 22$, $PB = 24$, $PC = 28$ corresponding to the curtain layers A, B, C, cf. Appendix.

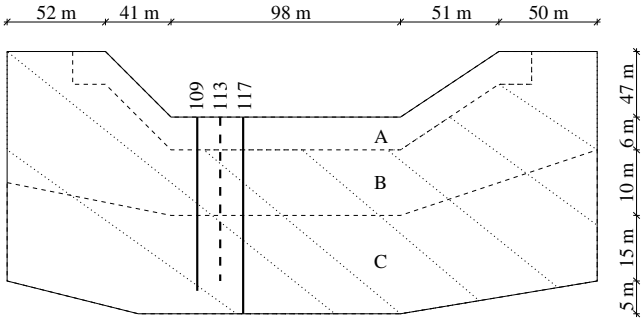

Fig. 1. Scheme of the Klimkówka dam grout curtain

2 Neural simulations

2.1 General remarks

The pattern set was examined by means of MLP type neural networks called in [4] Back-Propagation Neural Networks (BPNNs). Using different validation procedures [5] it was stated that the patterns are very inconsistent and that was why a decomposition of the problem was performed, i.e. three networks of different architecture were designed. These BPNNs were then used for the standard neural prediction, i.e. using crisp values for the inputs, outputs and NN parameters (weights and biases). Then the analysis was repeated by three Fuzzy Weight Neural Networks (FWNNs), corresponding to standard BPNNs formulated for the curtain layers.

The formulation of FWNN was described in [6] but because of a delay in publishing the Conference Proceedings a short description of this NN is given below.

2.2 Network FWNN

The Fuzzy Weight Neural Network (FWNN) is formulated on the base of the approach described in [7]. The main idea lies in the learning of the standard BPNN by a sequence of individual patterns. The set of neural parameters (synaptic weights and biases), called for short set of weights, can then be used for the formulation of the weight membership functions. A schematic algorithm of the FWNN formulation, taken from [6], is shown in Fig. 2.

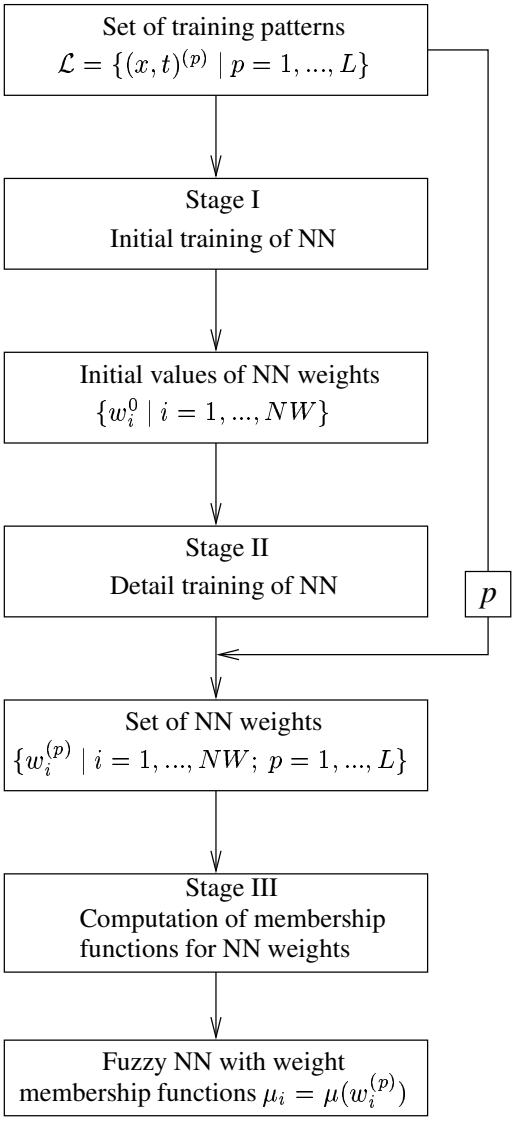

Fig. 2. Schematic algorithm of FWNN formulation

In Stage I the standard BPNN is trained on all training patterns L. The computed set of NN weights $\{w_i^0\}$ for $i = 1, \ldots, NNP$, where NNP is number of weights, is used at the next Stage II as a set of initial values. At Stage II the network is learnt L times for a sequence of single training pairs $(\mathbf{x}, \mathbf{t})^{(p)}$ starting from the same initial weights $\{w_i^0\}$. After the training is ended a set of weights is completed $\{w_{ip}\} = \{w_{i1}, \ldots, w_{iL}\}$ for each weight i. At Stage III the membership function $\mu_i = \mu(\{w_{ip}\})$ is formulated for each weight.

In [6] the formulation of membership functions was supported on pseudo-experimental cumulative functions. In the present paper we used triangular shape functions (in Fig. 3. the subscript i is omitted) as suggested in [7].

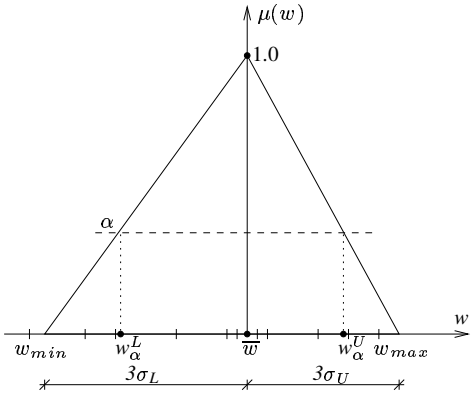

Fig. 3. Triangular membership function of a NN weight

After the membership functions are formulated for all the NN weights the FWNN neural network is ready for operation. In the operational phase the interval arithmetics is used with respect to α-cuts. FWNN can be used for the input-output mapping for the interval inputs $[x_j^L, x_j^U]_\alpha$, where j = 1,..., N are components of the input vector. In case of crisp inputs there are $x = x_j^L = x_j^U$ for each α. Independent of type of inputs (crisp or interval values) the FWNN output is always of interval type $[y_m^L, y_m^U]_\alpha$, i.e. a membership output function can be estimated by a set of discrete α-cuts.

2.3 Neural prediction of water absorption for the Klimkówka dam grout curtain

Results of measurements taken during the sealing process are listed in Appendix completed on the base of [3]. The measurements are split into three groups corresponding to the curtain layers A, B, C.

The total set of patterns $P = \{(\mathbf{x}, y)^{(p)} | p = 1, \ldots, P\}$ for $P = PA + PB + PC = 22 + 24 + 28 = 74$ is used to perform the mapping $\mathbf{x}^{(p)} \in \mathbf{R}^4 \rightarrow y^{(p)} \in \mathbf{R}^1$, optimal with respect to minimum of the RMSE measure

$$RMSE = \frac{1}{K}\sqrt{\frac{1}{S}\sum_{r=1}^{K}\sum_{p=1}^{S}(t_r^{(p)} - y_r^{(p)})^2}, \qquad (2)$$

where: $r = 1, \ldots, K$ – number of learning processes; $p = 1, \ldots, S$ – number of patterns; $t_r^{(p)}, y_r^{(p)}$ – target and computed (approximated) values of outputs, respectively; $S = L, T$ – number of training or testing patterns, respectively.

The total number of $P = S = 74$ patterns appeared to be small with respect to their density and distribution in the four dimension input space. That was why the cross-validation procedures corresponding to the families of BPNNs of structure 4-H-1, 4-H1-H2-1 did not give numerically efficient (low errors (2)) architectures of the BPNN networks. Much more efficient was decomposition of the simulation problem and formulation of three BPNNs, separately for each curtain layer.

The three sets PA, PB and PC have a scarce number of patterns. That is why the multifold cross-validation approach was applied [5]. Each set Pl was randomly split into $K = 10$ subsets Tlr, where $r = 1,\ldots, K$, containing 2-3 elements. Then for each layer l the subsets Tlr and their partitions Llr (i.e. $Tlr \cup Llr = Pl, Tlr \cap Llr = \emptyset$) are assumed to be the validation (testing) and estimation (training) sets, respectively. The training and testing processes were carried out $K = 10$ times for the sequence $r = 1,\ldots,10$. For each r the validation of the BPNN: 4-H-1 model was made in order to find an optimal number of sigmoidal neurons H_{opt} (linear neurons were used for outputs).

The above mentioned validation process was carried out by the MATLAB Neural Network simulator [8] using the Levenberg-Marquard learning method and, ending training at 60 epochs. As a result the following BPNN structures were designed: A) 4-2-1, B) 4-2-1, C) 4-4-1. Then the networks were also used for formulating FWNNs in the corresponding curtain layers.

3 Discussion of results

3.1 Crisp prediction of unit water absorption

The neural prediction is estimated with respect to each curtain layer. The errors of neural approximation are put together in Table 1. The number of learning processes in Formula (2) was fixed as $K = 10$ testing sets for the designed BPNNs: 4-Hl-1 in which the number of hidden neurons was validated as HA = 2, HB = 2, HC = 4. The following relative errors were also defined:

$$RE = |1 - y_r^{(p)}/t_r^{(p)}| \cdot 100\%, \quad (3)$$

$$REb = |1 - y_{rb}^{(p)}/t_{rb}^{(p)}| \cdot 100\%, \quad (4)$$

$$ARE = \frac{1}{K \cdot S} \sum_{r=1}^{K} \sum_{p=1}^{S} RE, \quad (5)$$

$$MREb = \max_p REb, \quad (6)$$

where: $rb \in [1, 10]$ – number of cross-validation corresponding to minimum of validation error in Tlr; $S = L, T, P$ – number of training, testing and total patterns $P = L + T$, respectively.

Errors	Curtain layer					
	A		B		C	
	L	T	L	T	L	T
RMSE*10^2	4.95	39.07	2.92	11.36	3.20	6.62
ARE[%]	62.3	292.4	39.2	87.0	8.2	183.2
RMSEb*10^2	5.82	0.79	4.61	0.60	0.22	0.26
AREb[%]	44.6	8.6	20.6	22.7	6.7	8.5
MREb[%]	186.7	9.8	72.3	34.8	26.6	20.9
Rb^2	0.957		0.929		0.960	
stϵ	5.56		4.42		0.23	

Table 1. Neural prediction errors of unit water absorption Q

On the basis of errors listed in Table 1 it is evident that the best neural prediction is obtained in the lower curtain layer C. This conclusion is confirmed by experimental histograms shown in Fig. 4. The histogram for layer C is unimodal with the prediction errors $REb \leq 20\%$. This does not relate to cases B, C for which histograms are bimodal and trimodal and majority of errors are within ranges $REb \approx 50, 90\%$, respectively.

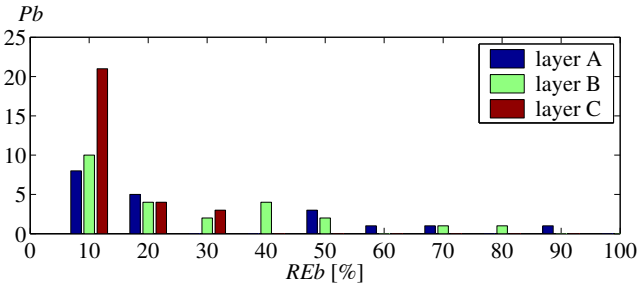

Fig. 4. Empirical histogram for P_b patterns in intervals $\Delta\, RE_b = 10\%$

Similar conclusions can be drawn on the base of experimental cumulative curves. In Fig. 5. the Success Ratio function is shown for:

$$SR(REb) = PS/P \cdot 100\%, \quad (7)$$

where: PS – number of pattern for which neural approximation error is not greater than REb, P – total number of patterns for the curtain layer considered. It is clear that for the curtain layer C the Success Ratio is $SR(REb = 10\%) = 75\%$. That means that about eighty percent of correct neural predictions is obtained within the error $REb \in [0, 10\%]$ and all neurally computed patterns will have approximation errors $REb \leq 30\%$. The neural prediction of the unit water absorption in secondary boreholes in the curtain layer B corresponds to $SR(REb = 10\%) = 42\%$, $SR(50\%) = 92\%$, $SR(100\%) = 100\%$. Much worse is the neural prediction in the layer A since the corresponding figures are $SR(10\%) = 36\%$, $SR(50\%) = 73\%$, $SR(100\%) = 86\%$.

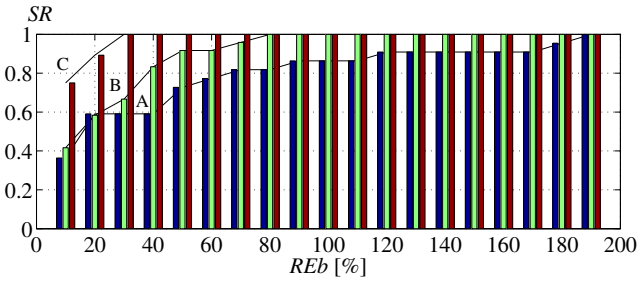

Fig. 5. Success Ratio functions $SR(REb)[\%]$ for curtain layers A, B, C

In the next Figs 6, 7, 8 the values of neurally computed unit water absorption QNN are shown vs. measured values QEX for each pattern associated with the layers C, B, A. The Figures correspond to the "best" BPNNs in sense of their validation. Statistical parameters, (i.e. coefficient of determination R^2 of sets $\{(QNN, QEX)^{(p)}\}$ and standard error stϵ for these sets) are written both in Figs 6, 7, 8 and in Table 1.

Selected average values of measured water and cement absorptions enable us to predict the water absorption in secondary boreholes with different accuracy. The deeper the soil layers, the better

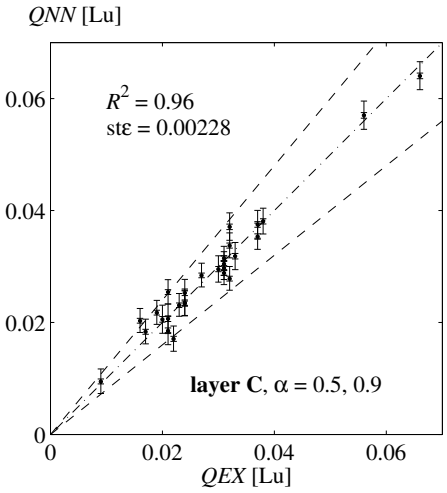

Fig. 6. Experimental vs predicted values in 20 percentage error cone

the neural prediction. In order to come near to reality of the sealing process a fuzzy prediction can be carried out. This goal can be partially achieved by the Fuzzy Weight Neural Networks (FWNNs).

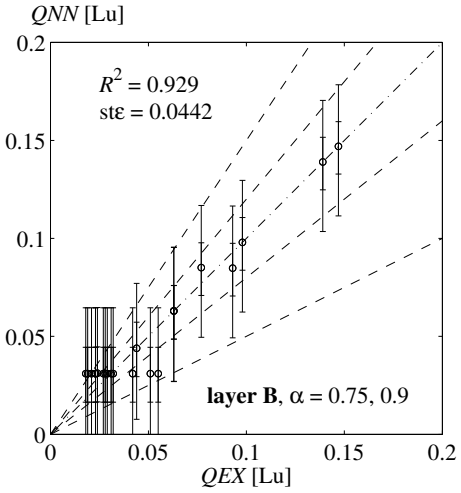

Fig. 7. Experimental vs predicted values in 20 and 50 percentage error cones

3.2 Fuzzy prediction of unit water absorption

Using initial values of NN weights from the above discussed BPNNs, fuzzy outputs were computed by means of corresponding FWNNs. In Figs. 9, 10, 11 the membership functions for selected outputs are shown, on the basis of computed interval values for cuts $\alpha = 0.0, 0.25, 0.5, 0.75, 0.9, 1.0$.

The above mentioned fuzzy approach is explored in neural prediction of interval values. In Fig. 6. there are shown intervals corresponding to $\alpha = 0.50$ which covers 79% of values measured in layer C (in case of $\alpha = 0.90$ the interval prediction covers 39% of values).

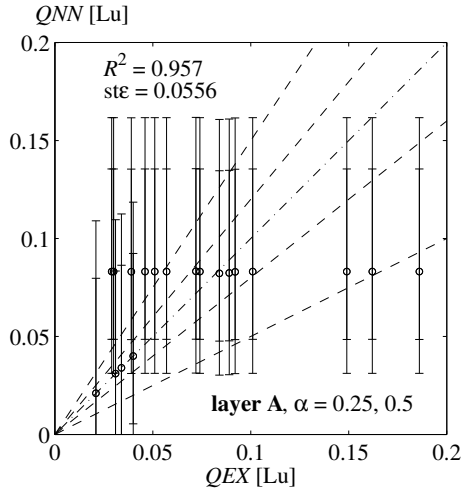

Fig. 8. Experimental vs predicted values in 20 and 50 percentage error cones

The intervals of $\alpha = 0.75, 0.90$ are span over 92% and 83% of water absorption values measured for the layer B, cf. Fig. 7. In case of layer A the $\alpha = 0.25$ intervals include 86% of measured values and $\alpha = 0.50$ gives covering of 59% of measured values, cf. Fig. 8.

The selected outputs correspond to patterns for which the errors of crisp neural approximation * are marked. The membership function in Fig. 9. corresponds to the pattern No 21 in layer C. The approximation by BPNN: 4-4-1 has relative error $REb(21) = 1.9\%$. It is visible that the measured value $Q_*(21) = 0.024$ can be bordered by the interval values $[0.0231, 0.0240]$ related to $\alpha = 0.90$.

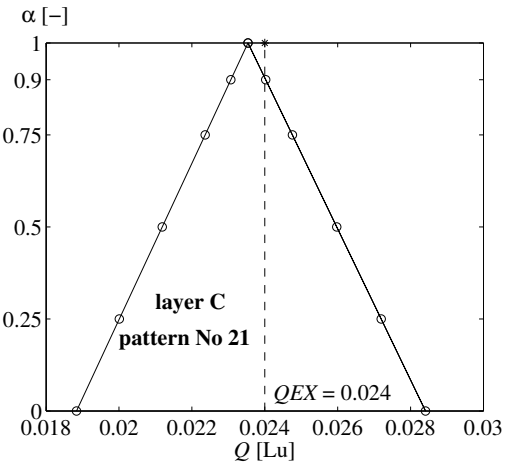

Fig. 9. Membership function for unit water absorption Q in the borehole No 21 of layer C

A similar approach but related to $Q_*(12) = 0.051$ in layer B is shown in Fig. 10, corresponding to the secondary borehole No 105 in layer B. The approximation by BPNN: 4-2-1 has relative error $REb(12) = 39.2\%$. The measured value $Q_*(12) = 0.051$ can be bordered by the interval values $[-0.0055, 0.0646]$ related to $\alpha = 0.75$.

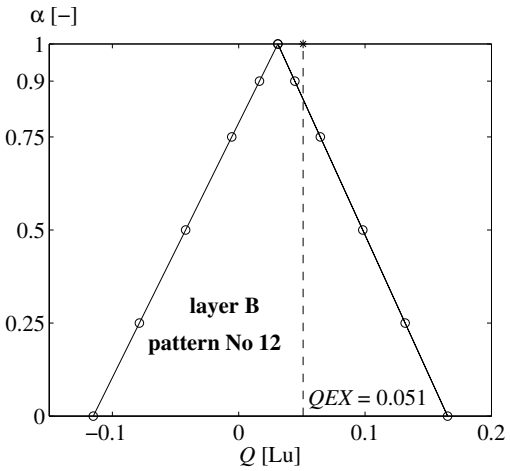

Fig. 10. Membership function for unit water absorption Q in the borehole No 12 of layer B

In Fig. 11 the membership function is shown for the borehold No 73 in layer A. The approximation by BPNN: 4-2-1 has relative error $REb(6) = 113.0\%$. The crisp values $Q_*(6) = 0.039$ is covered by the interval prediction $[0.0311, 0.1616]$ for $\alpha = 0.25$.

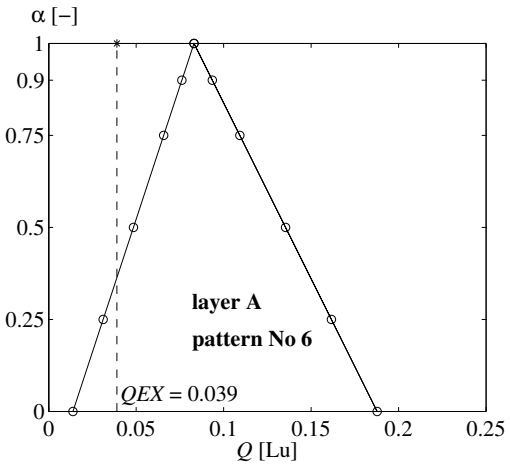

Fig. 11. Membership function for unit water absorption Q in the borehole No 6 of layer A

4 Conclusions

1. The sets of data related to unit water and cement absorptions in the primary and secondary boreholes in the analyzed dam grout curtain are very scarce and inconsistent.

2. A decomposition of the neural prediction was performed, i.e. different neural networks were formulated in each layer if the curtain layers.

3. The best, crisp type neural prediction by BPNN: 4-4-1 was obtained in the deeper layer C.

4. Interval prediction were performed by the fuzzy type networks FWNNs. In order to cover majority of experimental output values Q_* different α–cuts are needed ($\alpha = 0.25, 0.50$ in layer A, $\alpha = 0.75, 0.90$ in B and $\alpha = 0.50, 0.90$ in C).

5 Acknowledgement

Financial support by the Foundation for the Polish Science, Subsidy for Scientists No 13/2001 “Application of artificial neural networks to the analysis of civil engineering problems”, is gratefully acknowledged.

References

[1] Kutzner Ch., *Grouting of Rock and Soil*, A. A. Balkema, Rotterdam/Brookfield 1996.

[2] Głąb W., Jawański W. and Thiel K., *Research on the sealing of the dam foundation with cement-bentonite grouts* (in Polish), Institute of Building Organization and Mechanization, Warszawa 1965.

[3] *Geological documentation of the soil basement and grout curtain of the Klimkówka dam on the Ropa river*, (in Polish), “Hydrogeo”, Cracow, Dec. 1993.

[4] Waszczyszyn Z.(ed.), *Neural Networks in the Analysis and Design of Structures*, CISM Courses and Lectures No. 404, Springer, Wien - New York 1996.

[5] Haykin S., *Neural Networks – A Comprehensive Foundation*, Prentice Hall, Inc., Upper Saddle River, NJ 1999.

[6] Pabisek E., Jakubek M. and Waszczyszyn Z., A fuzzy neural network for the analysis of experimental structural mechanics problems, *Proc. 6th Intern. Conf. Neural Networks and Soft Computing ICNNSC 2002*, Zakopane, Poland, Springer, Heidelberg-Berlin, (in print).

[7] Ni S. H., Lu P. C. and Juang C. H., A fuzzy neural network approach to evaluation of slope failure potential, *Microcomputers in Civil Eng.*, **11** (1996), 59 - 66.

[8] Demuth H. and Beale M., *Neural Network Toolbox for Use with MATLAB*, User’s Guide, Version 4, The Mathworks, Natick MA 2001.

Appendix: Results of measurements in layers A, B, C of Klimkówka dam grout curtain.

Lr	No of pa.	No of bo.	Unit absorptions [Lu, kg/m]				
			Primary boreholes				Sec.bo.
			q_L	q_R	c_L	c_R	Q
A	1	25	1.045	0.194	195.5	121.7	0.461
	2	33	0.194	0.097	121.7	19.4	0.186
	3	49	0.284	0.326	512.7	489.6	0.029
	4	57	0.326	0.559	489.6	796.0	0.046
	5	65	0.559	0.157	796.0	182.8	0.040
	6	73	0.157	0.039	182.8	15.6	0.039
	7	81	0.039	0.437	15.6	358.8	0.074
	8	89	0.437	0.105	358.8	583.3	0.051
	9	96	0.105	0.052	583.3	70.9	0.034
	10	105	0.052	0.048	70.9	84.9	0.030
	11	113	0.048	0.097	84.9	153.8	0.101
	12	121	0.097	0.488	153.8	827.7	0.057
	13	129	0.488	0.242	827.7	374.0	0.084
	14	137	0.242	0.188	374.0	97.1	0.089
	15	145	0.188	0.496	97.1	927.2	0.072
	16	161	0.074	0.196	821.0	482.8	0.092
	17	169	0.196	0.318	482.8	58.8	0.031
	18	177	0.318	0.046	58.8	105.6	0.162
	19	185	0.046	0.034	105.6	15.5	0.149
	20	209	0.300	1.734	375.0	285.4	0.021
	21	217	1.734	0.432	285.4	114.6	0.821
	22	221	0.432	1.538	114.6	718.5	1.087
B	1	3	0.027	0.068	150.4	144.4	0.023
	2	7	0.068	0.164	144.4	206.2	0.077
	3	11	0.164	0.026	206.2	81.4	0.024
	4	17	0.026	0.038	81.4	108.0	0.023
	5	25	0.038	0.036	108.0	158.3	0.055
	6	49	0.109	0.078	530.0	486.0	0.029
	7	65	0.089	0.025	343.3	121.7	0.032
	8	73	0.025	0.012	121.7	0.0	0.021
	9	81	0.012	0.055	0.0	450.5	0.018
	10	89	0.055	0.081	450.5	261.3	0.027
	11	96	0.081	0.012	261.3	0.0	0.019
	12	105	0.012	0.036	0.0	84.9	0.051
	13	113	0.036	0.115	84.9	176.3	0.044
	14	121	0.115	0.108	176.3	270.0	0.093
	15	129	0.108	0.191	270.0	590.0	0.098
	16	137	0.191	0.171	590.0	935.0	0.063
	17	161	0.178	0.103	593.3	111.7	0.063
	18	169	0.103	0.021	111.7	11.7	0.042
	19	177	0.021	0.028	11.7	32.5	0.031
	20	185	0.028	0.070	32.5	343.3	0.028
	21	209	0.128	0.543	204.3	674.5	0.469
	22	217	0.543	0.228	674.5	250.0	0.139
	23	224	0.019	0.390	30.0	577.2	0.769
	24	228	0.390	0.191	577.2	543.8	0.147

Lr	No of pa.	No of bo.	Unit absorptions [Lu, kg/m]				
			Primary boreholes				Sec.bo.
			q_L	q_R	c_L	c_R	Q
C	1	3	0.042	0.093	63.5	249.0	0.021
	2	7	0.093	0.014	249.0	90.0	0.038
	3	17	0.020	0.012	34.0	0.0	0.031
	4	49	0.057	0.059	83.0	205.0	0.030
	5	57	0.059	0.032	205.0	27.5	0.017
	6	65	0.032	0.053	27.5	123.9	0.024
	7	73	0.053	0.038	123.9	69.6	0.021
	8	81	0.038	0.064	69.6	200.9	0.032
	9	89	0.064	0.065	200.9	91.3	0.022
	10	96	0.065	0.124	91.3	92.5	0.019
	11	105	0.124	0.043	92.5	13.3	0.031
	12	113	0.043	0.057	13.3	75.4	0.027
	13	121	0.057	0.046	75.4	34.2	0.032
	14	129	0.046	0.016	34.2	590.0	0.024
	15	137	0.016	0.040	590.0	273.6	0.023
	16	145	0.040	0.044	273.6	375.0	0.033
	17	153	0.044	0.062	375.0	252.8	0.020
	18	161	0.062	0.019	252.8	30.4	0.037
	19	169	0.019	0.023	30.4	0.0	0.031
	20	177	0.023	0.034	0.0	220.0	0.066
	21	185	0.034	0.111	220.0	441.7	0.024
	22	193	0.111	0.031	441.7	77.6	0.021
	23	201	0.031	0.028	77.6	86.4	0.032
	24	209	0.028	0.148	86.4	80.5	0.009
	25	217	0.148	0.112	80.5	243.9	0.031
	26	224	0.082	0.063	222.2	188.8	0.056
	27	228	0.063	0.009	188.8	0.0	0.016
	28	232	0.009	0.064	0.0	204.2	0.037

Abbreviations in the table heading:

Lr - layers of the curtain,

pa. - pattern,

bo. - borehole,

Sec.bo. - secondary borehole,

q_L, q_R - unit water absorptions in primary boreholes placed on the left and the right hand side of the secondary borehole,

c_L, c_R - unit cement absorption,

Q - unit water absorption in Sec.bo.